

# ChemComm

Chemical Communications

Accepted Manuscript

This article can be cited before page numbers have been issued, to do this please use: S. Watanabe, Y. Tsunekawa and K. Oyaizu, *Chem. Commun.*, 2025, DOI: 10.1039/D5CC03785A.



This is an Accepted Manuscript, which has been through the Royal Society of Chemistry peer review process and has been accepted for publication.

Accepted Manuscripts are published online shortly after acceptance, before technical editing, formatting and proof reading. Using this free service, authors can make their results available to the community, in citable form, before we publish the edited article. We will replace this Accepted Manuscript with the edited and formatted Advance Article as soon as it is available.

You can find more information about Accepted Manuscripts in the [Information for Authors](#).

Please note that technical editing may introduce minor changes to the text and/or graphics, which may alter content. The journal's standard [Terms & Conditions](#) and the [Ethical guidelines](#) still apply. In no event shall the Royal Society of Chemistry be held responsible for any errors or omissions in this Accepted Manuscript or any consequences arising from the use of any information it contains.

## COMMUNICATION

## Bleaching Effect of High Refractive Index Xylylic Poly(thiourea)s with “De-conjugated” Polarizable Hydrogen Bonds

Seigo Watanabe,<sup>a</sup> Yoshino Tsunekawa<sup>b</sup> and Kenichi Oyaizu<sup>\*a,b</sup>Received 00th January 20xx,  
Accepted 00th January 20xx

DOI: 10.1039/x0xx00000x

Poly(*p*-xylylene thiourea) (*pX*-PTU) exhibited high visible-light transparency ( $\%T \geq 99$ ), a high refractive index ( $n_D = 1.71$ ), and a reasonable Abbe number ( $\nu_D = 26$ ) owing to “de-conjugated” hydrogen bonds, which inhibit orbital interactions between the polarizable phenylene and thiourea units through sandwiched methylene spacers. Upon blending *pX*-PTU with all-aromatic poly(thiourea)s, their refractive index increased up to  $n_D = 1.80$ .

High refractive index polymers (HRIPs) typically exhibit refractive indices (RI) above 1.7 and are essential in various optoelectronic applications, including lighting devices, waveguides, and augmented/mixed reality (AR/MR).<sup>1–5</sup> To date, numerous HRIPs have been developed based on the Lorentz-Lorenz equation, which requires optimizing high polarizability and small molecular volume to achieve the desired RI and transparency at the target wavelength.<sup>2,4</sup> The most common HRIP categories are sulfur-containing polymers, such as poly(phenylene sulfide)s,<sup>4,6–10</sup> sulfur-rich polymers,<sup>3,11–13</sup> and poly(dithioacetal)s.<sup>14,15</sup> In particular, HRIPs with excessive sulfur content or conjugated  $\pi$ -skeletons achieve ultrahigh RI (over 1.8),<sup>11,16,17</sup> while they are colored due to the orbital interactions among  $\pi$ -skeletons and/or sulfur lone pairs (e.g.,  $n$ - $\pi$  interactions<sup>18</sup>). To address this empirical dilemma, we previously developed hydrogen-bonding (H-bonding) poly(phenylene sulfide)s to achieve both ultrahigh RI ( $n_D \sim 1.80$ – $1.85$ ) and visible-light transparency.<sup>19,20</sup> The key factor lies in the reduced free volume, which enhances the RI without compromising UV–visible (UV–vis) transparency. We further extended this concept to all-aromatic poly(thiourea)s (PTUs)

featuring multiple and polarizable H-bonds, exhibiting better RI ( $n_D \sim 1.7$ – $1.8$ ) and flexibility owing to strengthened PTU networks.<sup>21,22</sup> Also, other researchers have recently reported diverse high-RI PTU structures.<sup>23,24</sup> However, although all-aromatic PTU thin films are nearly colorless, their transparency remains low ( $\%T \geq 92$ , 1  $\mu\text{m}$  thick) owing to the direct coupling of polarizable thiourea and aromatic rings, which leads to excessive orbital interactions resulting in near-UV absorption and small Abbe numbers ( $\nu_D = 11$ – $18$ ).<sup>21</sup>

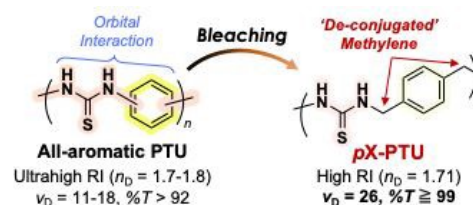


Fig. 1 Concept of the “de-conjugated” polarizable H-bonds: From all-aromatic PTU<sup>21</sup> (left: prior work) to *pX*-PTU (right: this work) to bleach high-RI PTUs.

In this study, we provide a new concept, termed “De-conjugated” polarizable H-bonds, to significantly enhance the transparency of high-RI PTUs (Fig. 1). The key design is poly(xylylene thiourea) (X-PTU), which contains a sandwiched methylene spacer that separates polarizable aromatic and thiourea groups, thereby inhibiting orbital interactions. In particular, *p*-substituted X-PTU (*pX*-PTU) exhibited amorphous and thermal properties comparable to those of the all-aromatic PTUs, while displaying improved transparency ( $\%T \geq 99$ ) and a higher Abbe number ( $\nu_D = 26$ ) with its high RI ( $n_D = 1.71$ ) maintained (Fig. 1, right). In addition, *pX*-PTU showed good miscibility with all-aromatic poly(1,3-phenylene-*alt*-1,4-phenylene thiourea) (*mpPh*-PTU), producing their simply blended transparent films with an enhanced  $T_g$  and well-balanced optical properties ( $T_g = 164$  °C,  $n_D = 1.80$ ,  $\nu_D = 17$ ). Overall, this study highlights the potential of “de-conjugated” H-bonding X-PTU and its polymer blends as a rational approach

<sup>a</sup> Research Institute for Science and Engineering, Waseda University, 3-4-1 Okubo, Shinjuku-ku, Tokyo 169-8555, Japan.  
E-mail: oyaizu@waseda.jp

<sup>b</sup> Department of Applied Chemistry, Waseda University, 3-4-1 Okubo, Shinjuku-ku, Tokyo 169-8555, Japan.

† Electronic Supplementary Information (ESI) available: experimental and synthetic procedures, characterization data, computational calculation, solid-state NMR results, and additional properties for the blends. See DOI: 10.1039/x0xx00000x



## COMMUNICATION

## ChemComm

to simultaneously maximize various properties (e.g., RI, Abbe, and transparency) for versatile optoelectronic polymers.

The X-PTUs were synthesized following our previous report,<sup>21</sup> involving the polycondensation of xylylene diamines (XDA) and 1,1-thiocarbonyl diimidazole (Scheme S1, S2). Two *m*- and *p*-substituted PTU isomers (**mX-PTU** and **pX-PTU**) were obtained as high-molecular-weight polymers ( $M_w \sim 10^5$ ), owing to the higher nucleophilicity of XDAs compared with that of all-aromatic diamines (Fig. 2a). The resulting X-PTUs were characterized by the  $^1\text{H}$  and  $^{13}\text{C}$  NMR spectroscopy, showing signals of thiourea, aromatic, and methylene groups (Fig. S1–S4). The IR spectra indicate two N–H conformations of thiourea ( $\nu_{\text{N-H(trans/trans):}} \sim 3270 \text{ cm}^{-1}$  and  $2\delta_{\text{N-H(cis/trans):}} \sim 3055 \text{ cm}^{-1}$ ), suggesting the presence of randomized H-bond networks (Fig. S5). Upon increasing temperature, the  $^1\text{H}$  variable-temperature (VT) NMR spectra of X-PTUs showed an upfield shift exclusively for the H-bonding amino signals (7.93–7.80 ppm) (Fig. 2b, Fig. S6). Notably, **pX-PTU** exhibited lower temperature dependence ( $-2.8 \times 10^{-3} \text{ ppm K}^{-1}$ ) than **mX-PTU** ( $-3.1 \times 10^{-3} \text{ ppm K}^{-1}$ ) and previously reported phenylene-PTUs ( $< -3.5 \times 10^{-3} \text{ ppm K}^{-1}$ )<sup>21</sup> (Fig. 2c). These results indicate that **pX-PTU** contains the strongest and high-temperature-resistant intermolecular H-bond network.

more temperature-resistant interchain H-bonds in the linear-shaped *p*-phenylene skeleton compared with the bent-shaped *m*-phenylene unit.

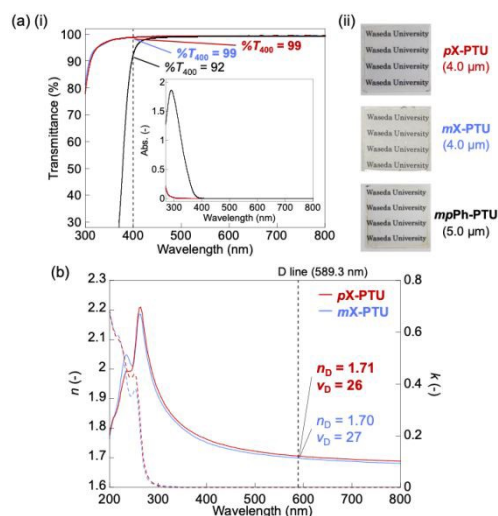


**Fig. 3** Optical properties of X-PTUs. (a) (i) Normalized UV-vis spectra for the films (thickness: 1  $\mu\text{m}$ ) of X-PTUs and **mpPh-PTU** (inset: UV-vis absorbance spectra of 0.1 mM solution in DMF). (ii) Photographs of PTU thin films on glass substrates and their thickness. (b) RI spectra:  $n$  (solid line) and  $k$  (dotted line).

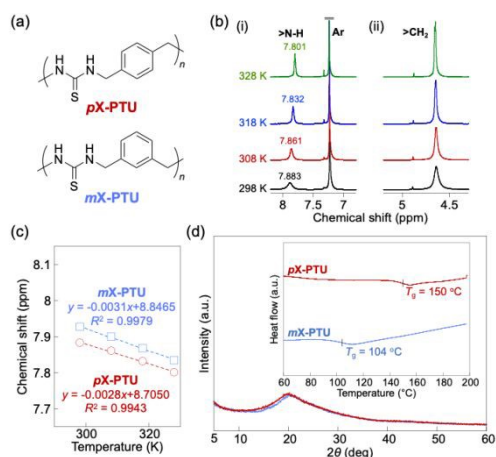


**Fig. 2** Properties of X-PTUs. (a) Chemical structures of **pX-PTU** and **mX-PTU**. (b)  $^1\text{H}$  VT-NMR of **pX-PTU**: (i) at 8.2–6.8 ppm (>N-H and aromatic signals), (ii) at 5.2–4.3 ppm (methylene signals). (c) Temperature dependence of >N-H chemical shifts in  $^1\text{H}$  VT-NMR. (d) XRD profiles (inset: DSC thermograms at a scan rate of  $20 \text{ }^\circ\text{C min}^{-1}$ ).

Regarding the crystalline properties, X-ray diffraction (XRD) profiles indicate an amorphous nature of X-PTUs, which can be attributed to the zig-zag H-bonds of the thiourea arrays (Fig. 2d). **X-PTU** exhibited good thermostability, with both an adequate  $T_g$  ( $> 100 \text{ }^\circ\text{C}$ ) and a high pyrolysis temperature ( $T_{d5} \sim 240\text{--}250 \text{ }^\circ\text{C}$ ), significantly surpassing those of phenylene-PTUs ( $T_g \sim 150 \text{ }^\circ\text{C}$ ,  $T_{d5} \sim 180 \text{ }^\circ\text{C}$ )<sup>21</sup> (Fig. 2d inset, Fig. S7). This superior thermostability can be attributed to the deconjugated X-PTU structure containing methylene spacers, which enhance the bond stability (dissociation energy) of C–N bonds, similar to the effect observed in aromatic/xylylic poly(dithiourethane)s.<sup>25</sup> Among the X-PTUs, **pX-PTU** showed a significantly higher  $T_g$  ( $150 \text{ }^\circ\text{C}$ ) than **mX-PTU** ( $T_g = 104 \text{ }^\circ\text{C}$ ), owing to the stronger and

Their optical properties were investigated to confirm the introduction effect of “de-conjugated” H-bonds (Fig. 3). The solution UV-vis spectra displayed that the X-PTUs exhibit superior visible-light transparency compared with **mpPh-PTU**, accompanied by a blue shift in near-UV absorption (Fig. 3a inset). This behavior can be attributed to the absence of orbital interactions between the lone pairs/ $\pi$ -electrons of the thioureas and phenylene rings upon the introduction of methylene spacers. To gain molecular-level insight, density functional theory (DFT) calculations were conducted on the model compounds of each polymer (Fig. S8). The orbital geometries of the phenylene-PTU models exhibited a widely distributed highest occupied molecular orbital (HOMO), which strongly overlapped with the lowest unoccupied molecular orbital (LUMO). In contrast, the X-PTU models showed a narrower distribution of continuous HOMO orbitals and less HOMO–LUMO geometry overlap. The estimated UV-vis spectra by time-dependent (TD) DFT calculations reproduced a pronounced blue shift in the near-UV absorption for the X-PTU models (Fig. S9). Therefore, the effect of “de-conjugated” methylene spacers in X-PTUs can be rationalized as the suppression of orbital interactions between thioureas and phenylene rings.

X-PTU thin films were also prepared via drop-casting or spin-coating, exhibiting colorless and visually transparent features (Fig. 3a), and the **pX-PTU** film displayed a fluorescence emission under UV irradiation (Fig. S10), as observed in typical PTUs.<sup>26</sup> Their UV-vis spectra display higher near-UV-vis transparency ( $\%T \geq 99$ ) than those of aromatic PTUs, owing to the bleaching effect in the X-PTUs (Fig. 3a (i), Fig. S11). Following the introduction of methylene spacers, the X-PTUs exhibited lower



RI ( $n_D = 1.71$  (**pX-PTU**) and  $1.70$  (**mX-PTU**)) than previously reported phenylene-PTUs ( $n_D \sim 1.8$ )<sup>21</sup> because of the decrease in the unit polarizability (Fig. 3b). However, their RI remained within the range of typical HRIPs,<sup>2,4</sup> while the Abbe numbers were markedly improved ( $\nu_D = 26$  (**pX-PTU**) and  $27$  (**mX-PTU**)) compared with those of the reported phenylene-PTUs ( $\nu_D \sim 11$ – $15$ )<sup>21</sup> and dimethyl-substituted PPS with a similar RI ( $n_D = 1.69$ ,  $\nu_D = 18$ ).<sup>27</sup> These trends follow the classical Kramers–Kronig relationship,<sup>28</sup> which explains that suppressing the near-UV absorption in X-PTUs results in a higher  $\nu_D$ . Furthermore, despite the low UV stability of aromatic PTUs ascribed to the presence of reactive C=S bonds<sup>29</sup> that induced lower transparency and RI (Fig. S12 and S13), the optical properties of **pX-PTU** were less deteriorated after the UV treatment than those for **mpPh-PTU**, thanks to the “de-conjugated” xylylene unit with less orbital interactions. In addition, there has been minimal change in RI and transparency of **pX-PTU** after the high-temperature or humid exposure (difference of % $T_{400} \sim 1\%$ ,  $n_D \sim \pm 0.01$ ) (Fig. S14–S17), attributed to the high hydrophobicity and rigidity ( $T_g$ ) of the aromatic main chain and the relatively hydrophobic H-bond properties<sup>30</sup> of the thiourea moieties to prevent the H-bond network destruction. Finally, the **pX-PTU** film displayed higher stress (17.2 MPa) and smaller strain (0.64 %) upon fracture than the previous aromatic PTU (12 MPa, 2.4 %) (Fig. S18), suggesting higher mechanical robustness due to the stronger H-bond nature of X-PTUs (Fig. 2c: vide supra).

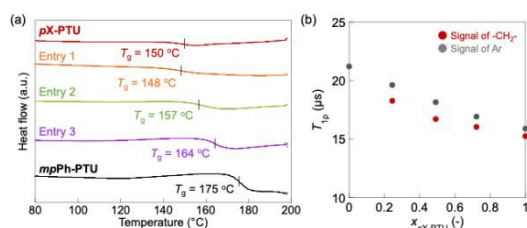


**Fig. 4** Miscibility studies of **pX-PTU** and **mpPh-PTU**. (a) DSC thermograms of the blends (2nd heating, scanning rate:  $20\text{ }^{\circ}\text{C min}^{-1}$ ). (b) Relationship between  $^1\text{H}$  Spin-lattice relaxation time ( $T_{1\rho}$ ) of the blends measured by solid-state CP-MAS  $^{13}\text{C}$  NMR and the molar ratio of **pX-PTU** ( $x_{pX-PTU}$ ).

In light of high-RI yet transparent optical properties of X-PTU, we further adjusted the thermostability and RI while maintaining high transparency by applying a blending strategy with different PTUs.<sup>31</sup> We selected **mpPh-PTU** as a blending counterpart because of its higher  $T_g$  ( $175\text{ }^{\circ}\text{C}$ ) and RI ( $n_D = 1.81$ ). Each PTU was blended by precipitating the DMF solution into methanol, yielding **pX-PTU/mpPh-PTU** blends with **pX-PTU** molar ratios of  $x_{pX-PTU} = 0.72, 0.49$ , and  $0.24$  (Fig. S19–S21). Their DSC thermograms display a single  $T_g$  that shifts to higher temperature as  $x_{pX-PTU}$  decreases (Fig. 4a), indicating good miscibility between each PTU with 10–20 nm scale homogeneity.<sup>32</sup> To further elucidate their miscibility on a further smaller scale, we conducted cross-polarization/magic angle spinning (CP/MAS)  $^{13}\text{C}$  NMR on the **pX-PTU/mpPh-PTU** blends (Fig. S23–S27). In short,  $^1\text{H}$  spin-lattice relaxation time ( $T_{1\rho}$ ) was determined from two areas, aromatic (ca. 150–100 ppm) and methylene (ca. 55–35 ppm) signals, for each composition (Fig. S28). While those  $T_{1\rho}$ s did not match perfectly,

they shifted proportionally with  $x_{pX-PTU}$ , confirming interdomain interactions between **pX-PTU** and **mpPh-PTU** in the blended matrices (Fig. 4b, Table S1). Therefore, although those PTUs were phase-separated on a 3–4 nm scale detectable by CP/MAS NMR measurements, they are miscible on a scale below 20 nm, as indicated by the  $T_g$  shifts observed in the DSC results.

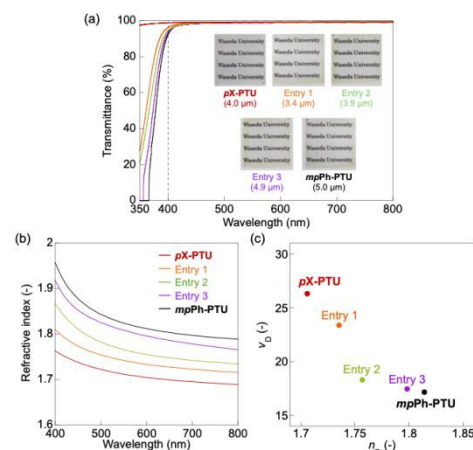


**Fig. 5** Optical Properties of the films of the **pX-PTU/mpPh-PTU** blends. (a) Normalized UV-vis spectra (film thickness:  $1\text{ }\mu\text{m}$ ) (inset: photographs and thickness of the films). (b) RI spectra in the visible-light region (for overall spectra, see Fig. S32). (c)  $n_D$  versus  $\nu_D$ .

The drop-cast **pX-PTU/mpPh-PTU** blend films were visibly transparent and exhibited no aggregation, further confirming the good miscibility of the PTUs (Fig. 5a inset). The UV-vis spectra of the blend films showed good transparency (94–96 %T for  $1\text{ }\mu\text{m}$  thickness), falling between the values of the individual PTUs regardless of the film thickness (Fig. 5a, Table S2, and Fig. S29–S31). These results demonstrated the bleaching effect with improved near-UV transparency upon increasing  $x_{pX-PTU}$ . Their ATR-IR spectra showed a consistent peak shift of the H-bonded N–H vibration modes ( $\nu_{N-H}$  and  $2\delta_{N-H}$ ) (Fig. S32), indicating the presence of homogeneous H-bond networks even in the blended states without any macroscopic phase separation.

The RI spectra also followed consistent shifts in  $n_D$  and  $\nu_D$  corresponding to the blending ratio (Fig. 5b). In short, the **pX-PTU/mpPh-PTU** blend with higher  $x_{pX-PTU}$  exhibited a lower RI and higher  $\nu_D$  across the entire visible-light region, aligning well with the empirical RI–Abbe trade-off relationship<sup>33</sup> (Fig. 5c). The extinction coefficient ( $k$ , the imaginary part of the complex RI) also decreased with higher  $x_{pX-PTU}$ , demonstrating the bleaching effect upon the **pX-PTU** introduction (Fig. S33). Summarizing above, **pX-PTU** was miscible with the aromatic PTU on a 10–20 nm scale, and their polymer blends produced transparent films with enhanced thermostability and RI. In particular, entry 3 ( $x_{pX-PTU} = 0.24$ ; Table 1) showed the best balance of thermal and optical properties among the PTU family, exhibiting a high  $T_g$  ( $164\text{ }^{\circ}\text{C}$ ) and ultrahigh RI ( $n_D = 1.80$ ), while simultaneously achieving a reasonable Abbe number ( $\nu_D = 17$ ) and visible light transparency (94 %T,  $1\text{ }\mu\text{m}$  thickness).

In summary, we demonstrated the X-PTU family as an HRIP substructure with unprecedented near-UV–vis transparency





and Abbe numbers (e.g., **pX-PTU**:  $n_D = 1.71$ ,  $v_D = 26$ ). The key molecular design lies under the “de-conjugated” H-bonds, which involves separating the polarizable aromatic and thiourea moieties with sandwiched methylene spacers to inhibit their orbital interactions while maintaining high polarizability and H-bond density. In particular, **pX-PTU** exhibited adequate thermostability ( $T_g = 150$  °C) and good miscibility with **mpPh-PTU** on a 10–20 nm scale, and their blended films demonstrated adjustable thermal and optical properties. To our knowledge, this study is the first to demonstrate how orbital interactions in an HRIP bearing polarizable H-bonds affect the overall optical properties. Further, miscible polymer blending is verified as a simple strategy to adjust thermal and optical properties. Expanding this concept to diverse polarizable H-bond containing HRIP skeletons (e.g., poly(thioamide)s<sup>23,34</sup> and poly(sulfamide)s<sup>35</sup>) leads to further design of optical polymers surpassing the empirical RI-Abbe trade-off limit.

This work was partially supported by Grants-in-Aid for Scientific Research (Nos. 21H04695, 22K18335, and 25K18083) from MEXT, Japan, the Satomi Scholarship Foundation, and ENEOS Tonen General Research/Development Encouragement & Scholarship Foundation.

## Conflicts of interest

There are no conflicts to declare.

## Data availability

The data supporting this article have been included as part of the Supplementary Information.

## Notes and references

- J.-G. Liu and M. Ueda, *J. Mater. Chem.*, 2009, **19**, 8907–8919.
- T. Higashihara and M. Ueda, *Macromolecules*, 2015, **48**, 1915–1929.
- T. S. Kleine, R. S. Glass, D. L. Lichtenberger, M. E. Mackay, K. Char, R. A. Norwood and J. Pyun, *ACS Macro Lett.*, 2020, **9**, 245–259.
- S. Watanabe and K. Oyaizu, *Bull. Chem. Soc. Jpn.*, 2023, **96**, 1108–1128.
- A. Nishant, K.-J. Kim, S. A. Showghi, R. Himmelhuber, T. S. Kleine, T. Lee, J. Pyun and R. A. Norwood, *Adv. Opt. Mater.*, 2022, **10**, 2200176.
- Y. Suzuki, K. Murakami, S. Ando, T. Higashihara and M. Ueda, *J. Mater. Chem.*, 2011, **21**, 15727–15731.
- K. Nakabayashi, T. Imai, M.-C. Fu, S. Ando, T. Higashihara and M. Ueda, *Macromolecules*, 2016, **49**, 5849–5856.
- M.-C. Fu, Y. Murakami, M. Ueda, S. Ando and T. Higashihara, *J. Polym. Sci. A Polym. Chem.*, 2018, **56**, 724–731.
- S. Watanabe, Y. Tsunekawa, T. Takayama and K. Oyaizu, *Macromolecules*, 2024, **57**, 2897–2904.
- S. Watanabe, Z. An, H. Nishio, Y. Tsunekawa and K. Oyaizu, *J. Mater. Chem. C*, 2025, **13**, 7933–7942.
- J. J. Griebel, S. Namnabat, E. T. Kim, R. Himmelhuber, D. H. Moronta, W. J. Chung, A. G. Simmonds, K.-J. Kim, J. van der Laan, N. A. Nguyen, E. L. Dereniak, M. E. Mackay, K. Char, R. S. Glass, R. A. Norwood and J. Pyun, *Adv. Mater.*, 2014, **26**, 3014–3018.
- D. H. Kim, W. Jang, K. Choi, J. S. Choi, J. Pyun, J. Lim, K. Char and S. G. Im, *Sci Adv*, 2020, **6**, eabb5320.
- K.-S. Kang, C. Olikagu, T. Lee, J. Bao, J. Molineux, L. N. Holmen, K. P. Martin, K.-J. Kim, K. H. Kim, J. Bang, V. K. Kumirov, R. S. Glass, R. A. Norwood, J. T. Njardarson and J. Pyun, *J. Am. Chem. Soc.*, 2022, **144**, 23044–23052.
- S. Watanabe, T. Yano, Z. An and K. Oyaizu, *ChemSusChem*, 2025, **18**, e202401609.
- J.-Z. Zhao, T.-J. Yue, B.-H. Ren, Y.-X. Ma, X.-B. Lu and W.-M. Ren, *J. Am. Chem. Soc.*, 2025, **147**, 19762–19769.
- X. Wu, J. He, R. Hu and B. Z. Tang, *J. Am. Chem. Soc.*, 2021, **143**, 15723–15731.
- M. Lee, Y. Oh, J. Yu, S. G. Jang, H. Yeo, J.-J. Park and N.-H. You, *Nat. Commun.*, 2023, **14**, 2866.
- A. Fukazawa, Y. Toda, M. Hayakawa, A. Sekioka, H. Ishii, T. Okamoto, J. Takeya, Y. Hijikata and S. Yamaguchi, *Chem. Eur. J.*, 2018, **24**, 11503–11510.
- S. Watanabe and K. Oyaizu, *Macromolecules*, 2022, **55**, 2252–2259.
- S. Watanabe, H. Nishio, T. Takayama and K. Oyaizu, *ACS Appl. Polym. Mater.*, 2023, **5**, 2307–2311.
- S. Watanabe, L. M. Cavinato, V. Calvi, R. van Rijn, R. D. Costa and K. Oyaizu, *Adv. Funct. Mater.*, 2024, **34**, 2404433.
- S. Watanabe, Y. Tsunekawa and K. Oyaizu, *Macromol. Chem. Phys.*, 2025, 2400456.
- Y. Huang, R. Hu and B. Z. Tang, *Macromolecules*, 2024, **57**, 6568–6576.
- Y. Yu, W. Chen, R. Hu and B. Z. Tang, *Polym. Chem.*, 2025, **16**, 1509–1518.
- Y. Yoshida and T. Endo, *J. Polym. Sci. A Polym. Chem.*, 2018, **56**, 2255–2262.
- J. Zhang, F. Ye, J.-L. Huo, J.-W. Peng, R.-R. Hu and B. Z. Tang, *Chin. J. Polym. Sci.*, 2023, **41**, 1563–1576.
- S. Watanabe, T. Takayama, H. Nishio, K. Matsushima, Y. Tanaka, S. Saito, Y. Sun and K. Oyaizu, *Polym. Chem.*, 2022, **13**, 1705–1711.
- M. Fox, *Optical Properties of Solids*, OUP Oxford, 2001, vol. 70.
- S. Yoo, H. Park, Y. S. Kim, J. C. Won, D.-G. Kim and Y. H. Kim, *J. Mater. Chem. C*, 2021, **9**, 77–81.
- K. Kikkawa, Y. Sumiya, K. Okazawa, K. Yoshizawa, Y. Itoh and T. Aida, *J. Am. Chem. Soc.*, 2024, **146**, 21168–21175.
- Y. Fujisawa, Y. Nan, A. Asano, Y. Yanagisawa, K. Yano, Y. Itoh and T. Aida, *Angew. Chem. Int. Ed Engl.*, 2023, **62**, e202214444.
- A. Asano and T. Kurotu, *J. Mol. Struct.*, 1998, **441**, 129–135.
- S. Watanabe, T. Takayama and K. Oyaizu, *ACS Polym Au*, 2022, **2**, 458–466.
- Y. Hu, L. Zhang, Z. Wang, R. Hu and B. Z. Tang, *Polym. Chem.*, 2023, **14**, 2617–2623.
- J. W. Wu, R. W. Kulow, M. J. Redding, A. J. Fine, S. M. Grayson and Q. Michaudel, *ACS Polym. Au*, 2023, **3**, 259–266.



**Data availability statement**

The data supporting this article have been included as part of the Supplementary Information.

